Bioprinting of tissue engineering scaffolds

Patrick Rider[1], Željka Perić Kačarević[2] iD **, Said Alkildani[3],
Sujith Retnasingh[4] and Mike Barbeck[1,5]**

Abstract

Bioprinting is the process of creating three-dimensional structures consisting of biomaterials, cells, and biomolecules. The current additive manufacturing techniques, inkjet-, extrusion-, and laser-based, create hydrogel structures for cellular encapsulation and support. The requirements for each technique, as well as the technical challenges of printing living cells, are discussed and compared. This review encompasses the current research of bioprinting for tissue engineering and its potential for creating tissue-mimicking structures.

Introduction

Tissue engineering is a subcategory of regenerative medicine aimed at repairing or replacing damaged and impaired tissues. Conventional methods used for manufacturing tissue engineered scaffolds lack the ability to produce highly repeatable designs with precise, well-defined micro- and nanoscale structures.[1,2]

Three-dimensional (3D) printing (or additive manufacturing (AM)) is capable of producing scaffolds fabricated to patient-specific requirements. Bioprinting uses AM techniques to produce 3D structures consisting of living cells, biomaterials, and active biomolecules. One of the main advantages of bioprinting is the homogeneous distribution of cells,[3] which can otherwise be an issue when seeding cells onto large tissue scaffolds. First patented attempts of bioprinting started with filling cartridges of table-top inkjet printers with bioinks, which mainly consisted of cell-laden hydrogels.[4] Although research using inkjet technology was an early adapter for bioprinting, many other AM techniques have also been utilized. Currently used bioprinting techniques are based on inkjet, extrusion, or laser AM technology.

Each bioprinting technique primarily uses hydrogels as a basis for printing in the form of a bioink. Hydrogels are materials with 3D molecular networks that have a high water intake. Their high water content allows for cell entrapment and encapsulation without inflicting damage to the cells. Therefore, hydrogels are most commonly used as

the base material for bioinks.[5] The main parameters for developing a bioink are as follows: the choice of material, its concentration, and chemical properties. The main considerations for bioinks have been explored in a review by Prendergast et al.[6] This review will cover the main concepts behind each bioprinting technique, as well as current research into the development of bioprinted tissue scaffolds. An overview of the most significant research comparing different tissues and each bioprinting technique is shown in Table 1.

[1]botiss biomaterials, Berlin, Germany
[2]Department of Anatomy Histology, Embryology, Pathology Anatomy and Pathology Histology, Faculty of Dental Medicine and Health, Josip Juraj Strossmayer University of Osijek, Osijek, Croatia
[3]Department of Biomedical Engineering, Faculty of Applied Medical Sciences, German Jordanian University, Amman, Jordan
[4]Institute for Environmental Toxicology, Martin-Luther-Universität Halle-Wittenberg and Faculty of Biomedical Engineering, Anhalt University of Applied Science, Köthen, Germany
[5]Department of Oral and Maxillofacial Surgery, University Hospital Hamburg-Eppendorf, Hamburg, Germany

Corresponding author:
Željka Perić Kačarević, Department of Anatomy Histology, Embryology, Pathology Anatomy and Pathology Histology, Faculty of Dental Medicine and Health, Josip Juraj Strossmayer University of Osijek, 31000 Osijek, Croatia.
Email: zeljkapericc@gmail.com

Table 1. Overview of the most significant research comparing different tissues and bioprinting techniques.

Bioink	Cell type	Results	Reference
Skin			
Inkjet-based			
Collagen type I	Fibroblasts Keratinocytes	Developed a multilayered skin model with multiple cell types	Cui and Boland[7]; Christensen et al.[8]
PEG	Fibroblasts Keratinocytes	Developed an all-in-one solution for printing skin	Ku[9]
Collagen	HMVECs NHDF	Successfully transplanted printed skin grafts into mice	Lee et al.[10]
Fibrinogen–collagen	MSCs	Successfully demonstrate in-situ printing to repair full thickness skin wounds on the backs of mice	Lee et al.[11]
Extrusion-based			
PDMS	Fibroblasts Keratinocytes	Developed a multilayered epidermal skin layer	Cui and Boland[7]
PCL	HDFs HEKs	Developed a new 3D cell printing strategy to fabricate a 3D skin tissue model	Zhu and Liang[12]
Laser-assisted			
Alginate + blood plasma	Fibroblasts Keratinocytes hMSCs	Performed accurate positioning of multiple cell types	Lim et al.[13]
Bone and cartilage			
Inkjet-based			
Fibrin/collagen hydrogel	Chondrocytes	Successfully demonstrated cartilage formation when implanted in mice	Xu et al.[14]
PEGDMA	Chondrocytes	Used FGF-2 and FGF-2/TGF-β1 doped scaffolds for cartilage development	Cui et al.[15]
PEGDMA	Chondrocytes	Demonstrated potential for in-situ printing	Cui et al.[16]
Extrusion-based			
Matrigel and alginate	EPCs MSCs	Observed bone-like formation in the scaffold 6 weeks after implantation in mice	Ozbolat and Hospodiuk[17]
PCL	hASCs	Performed craniofacial regeneration	Bishop et al.[18]
GelMA and HAMa	IPFP cells	Successfully demonstrated reconstruction of chondral defects	Fedorovich et al.[19]
GelMA	Chondrocytes	Cartilaginous tissue was observed after 4 weeks when implanted in mice	Hung et al.[20]
PCL-alginate gel	Chondrocytes	Cartilaginous tissue formation was observed in the scaffold when implanted in subcutaneous spaces of mice	Oussedik et al.[21]
Stereolithography			
GelMA and nHA	Osteoblasts hMSCs	Developed a 3D bone-mimicking model to study metastasis	Zhou et al.[22]
GelMA and collagen type I	hMSCs	Developed a method to minimize oxygen inhibition	Tzeng et al.[23]
GelMA + PEGDA + TGF-β1	hMSCs	Fabricated scaffolds from a precursor hydrolgel, in which cells and nanospheres were suspended	Weiß et al.[24]
Laser-assisted			
Sodium alginate	Osteosarcoma cells (MG63)	Evaluated the effect of 3D positioning of cells on PCL biopapers	Morris et al.[25]
N.A.	HUVECs	Performed positioning of enothelial cells within osseous biopapers to induce vascularization	Williams et al.[26]
Neural			
Inkjet-based			
Phosphate-buffered saline	CHO and rat embryonic motoneurons	Demonstrated successful printing of neural cells using a thermal inkjet printer	Xu et al.[27]
Dulbecco's modified Eagle's medium	Primary rat embryonic neurons	Demonstrated that there was no difference in cell survival rate and neurite growth between printed and non-printed cells	Xu et al.[28]

Table 1. (Continued)

Bioink	Cell type	Results	Reference
Extrusion-based			
PU	NSCs	Repaired damaged nervous system in adult zebra fish	Chung et al.[29]
N.A.	BMSCs	Successfully fabricated purely cellular nerve grafts	Pranzo et al.[30]; Kundu et al.[31]
Stereolithography			
GelMA and graphene nanoplatelets	hNSCs	Fabricated 3D scaffolds with a homogeneous distribution of cells and graphene nanoplatelets	Lu et al.[32]
Corneal			
Extrusion-based			
Sodium alginate and collagen	Corneal keratinocytes	Demonstrated cell viability of KC remained 90% after day 1 of post printing	Kim et al.[33]
Laser-assisted			
Collagen I + recombinant laminin	hESC-LESCs hASCs	Performed accurate positioning of multiple cell types	Park et al.[34]
Cardiac			
Inkjet-based			
Alginate	Cardiomyocytes	Successfully printed half heart shape with two connected ventricles, showed contract rhythm under electric stimulation	Lorber et al.[35]
Alginate and gelatin gel	Endothelial cells	Printed tubes, branched tubes, hollow cones, and capillaries with a microscopic porosity	Xu et al.[36]
Fibrin hydrogel	HMVEC	Achieved confluent cell linings with a ring-shaped microvasculature	Nakamura et al.[37]
Sodium alginate	NIH-3T3	Printed vascular shapes using a liquid support material	Boland et al.[38]
Extrusion-based			
GelMA	iPSCs	Developed a microfibrous scaffold capable of spontaneous and synchronous contraction	Hsieh et al.[39]
Me-HA	HAVIC	Printed scaffold began to be remodeled after 3 days in culture	Hsu et al.[40]
Muscular			
Extrusion-based			
PEGDA and GelMA	NIH-3T3 and C2C12	Successfully implanted in rats	Dhariwala et al.[41]
Stereolithography			
PEGDA	ESCs and C2C12	Employed dielectrophoresis in cell patterning prior to printing	Pati et al.[42]
Dental			
Extrusion-based			
GelMA and PEG	PDLSCs	Successfully demonstrated an array of hydrogel with high cell viability of 94%	O'Connell et al.[43]
PCL and β-TCP	–	Successfully demonstrated the reconstruction of maxillary bone defect in a dog	Schuurman et al.[44]

PEG: polyethylene glycol; 3D: three-dimensional; HMVEC: human microvascular endothelial cell; NHDF: neonatal human dermal fibroblast; MSC: mesenchymal stem cell; PDMS: polydimethylsiloxane; PCL: polycaprolactone; HDF: human dermal fibroblast; HEK: human epidermal keratinocyte; PEGDMA: poly(ethylene glycol) dimethacrylate; FGF: fibroblast growth factor; TGF: transforming growth factor; EPC: endothelial progenitor cell; hASC: human adipose–derived stem cell; HAMa: hyaluronic acid-methacrylate; GelMA: gelatin-methacrylamide; IPFP: infrapatellar fat pad; PEGDA: poly(ethylene glycol) diacrylate; CHO: Chinese hamster ovary; PU: polyurethane; NSC: neural stem cell; hMSC: human mesenchymal stem cell; BMSC: bone marrow stem cell; hNSC: human neural stem cell; KC: keratinocyte; LESC: limbal epithelial stem cell; TCP: tricalcium phosphate; iPSC: induced pluripotent stem cell; Me-HA: methacrylated hyaluronic acid; HAVIC: human aortic valvular interstitial cell; PDLSC: periodontal ligament stem cell.

Techniques

Inkjet

Inkjet-based bioprinting is a non-contact printing technique in which droplets of dilute solutions are dispensed, driven by thermal, piezoelectric, or microvalve processes.

Inkjet bioprinting technology is based on the conventional inkjet process used by desktop inkjet printers, whereby individual droplets are used to pattern a substrate. The concept of inkjet printing was first developed in the early 1950s by Epson, Hewlett-Packard (HP), and Canon; however, it was not until 2003 before the first patent for a

modified inkjet printer for bioprinting of viable cells was awarded.[3,45,46] A structure is formed by continuously depositing droplets at predesigned points, enabling a structure with irregular shapes to be fabricated easily.[47] High spatial resolution can be achieved between 50 and 300 μm;[27,47] however, cell aggregation within the bioink can change droplet formation and trajectory, thereby reducing print quality.[48] Despite the many benefits of using inkjet technology, the use of low-concentration solutions can be a limiting factor when building up material into a 3D structure.[47] Collectively, inkjet printing has great potential in tissue engineering and regenerative medicine.

Cartilage and bone tissue. To produce a cartilage tissue scaffold that was suitable for load-bearing applications, Xu et al.[14] inkjet-printed rabbit articular chondrocytes suspended in a fibrin–collagen hydrogel onto an electrospun polycaprolactone (PCL) matrix. The scaffolds were fabricated by alternatively printing a layer of electrospun PCL fibers followed by a layer of chondrocytes/fibrinogen/collagen suspension. The inclusion of the PCL (M_n ~42,500, 10% wt/vol.) fibers within the natural polymer gel improved the mechanical properties. The PCL composite scaffold had a Young's modulus of 1.76 MPa and an ultimate tensile strength of 1.11 MPa compared to the natural polymer gel alone, which had a Young's modulus of 0.41 MPa and an ultimate tensile strength of 0.26 MPa. Cell viability of the printed cells, calculated by a comparison of living cells to total number of cells, was 81.58% ± 3.46% 1 week after printing. Scaffolds implanted subcutaneously in immunodeficient mice over an 8-week period developed a dense, well-organized collagen, not present in the control group (unseeded scaffolds). The cartilage tissue formation within the bioprinted scaffolds appeared histologically similar to normal elastic cartilage.

Scaffolds were fabricated by Cui et al.[15] using human chondrocytes suspended in a poly(ethylene glycol) dimethacrylate (PEGDMA) solution. The PEGDMA solution was polymerized using ultraviolet (UV) light during the printing process. Viability of the human chondrocytes after printing was 84.9% ± 2.2%. Scaffolds were cultured in cell culture medium, supplemented with either fibroblast growth factor-2 (FGF-2) or transforming growth factor-β1 (TGF-β1). TGF-β1 is used to maintain chondrocyte phenotype, while FGF-2 is used for chondrocyte monolayer expansion. The compressive moduli of the hydrogels reduced with the inclusion of cells and were dependent on cell density; however, compressive moduli increased with time spent in cell culture. Culturing with FGF-2/TGF-β1 supplemented medium was shown to be the most beneficial for cartilage development.

Cui et al.[16] also investigated the possibility for printing in situ. Using the same printing method as before, scaffolds were printed either separately or directly into osteochondral plugs that had been harvested from bovine femoral condyles. The printed scaffolds had a compressive modulus of 395.73 ± 80.40 kPa, similar to natural human collagen. By polymerizing the scaffold as each layer was printed, cellular exposure to UV radiation was reduced by more than 80% compared to manual hydrogel scaffold polymerization that normally requires >10 min UV exposure. Compared to the control of a cast scaffold, cell viability of the printed cells was 26% higher. The inclusion of cells into the polymer matrix made the scaffolds ~20% more flexible, possibly due to the cells absorbing some of the compressive forces. Scaffolds that were printed directly into the bovine femoral condyles defects had enhanced tissue integration compared to non-printed cell-laden hydrogels. The improved tissue integration for scaffolds printed directly into the defect, along with a fabrication timing of 108 s, makes the bioprinting process a viable option for in-situ applications; however, the achieved compressive modulus of the scaffolds is significantly lower than that of human articular cartilage of the lower limbs, which range between 4.5 and 11.8 MPa.[49] Therefore, further structural development of the scaffold would need to be considered before human implantation.

Neural tissue. To establish the ability of thermal inkjet printing for depositing mammalian cells, Chinese hamster ovary (CHO) and rat embryonic motoneuron cells were printed, suspended in a phosphate-buffered saline (PBS).[27] After printing, the cells maintained a healthy morphology. The CHO cells proliferated into a confluent layer, while the rat embryonic motoneuron cells proliferated and exhibited a polarized morphology. CHO cell lysis was evaluated immediately after printing and indicated that ~8% of the cells were damaged due to the printing process. Overall, the study demonstrated the potential for inkjet printing to deposit cells into tissue scaffolds.

Further experiments were conducted with rat primary embryonic hippocampal and cortical neurons.[28] Viability of the cells was 74.2% ± 6.3%, which maintained their basic function, phenotype, and electrophysiological properties. The printed cortical cells developed into mature neurons, while both types of cells could produce action potentials.

Lorber et al.[35] were the first group to print cells from the mature adult nervous system. Printing with adult cells is more challenging, as adult neural cells are more prone to damage and are less able to regenerate. Using a high-speed, image-capture setup, it was observed that during droplet ejection, the cells did not undergo major distortion and hence destruction caused by shear forces. There was no difference in cell survival rate and neurite growth between printed and non-printed cells. The glia cells retained their ability to support the growth of the retinal ganglion cells.

Tse et al.[50] were the first to print a combination of both neuronal and supportive glial cells. Not only did the

printed cells maintain high viabilities, >86% for neuronal cells and >89% for Schwann cells, but more importantly, the printed neuronal cells exhibited earlier and longer neurite growth in comparison with the non-printed cells. By demonstrating the successful printing of both the neuronal and glial cells, the potential for producing a large tissue scaffold with a complete neural network becomes a greater possibility and could have massive potential for the repair of large-area, full-thickness skin burns.

Cardiac and vascular tissue. Initial work into printing cardiac tissue was performed using alginate hydrogel and primary feline adult and human H1 cardiomyocytes.[36] Xu et al. printed a half heart shape that had a 1-cm inner diameter and two connected ventricles. In cell culture, the cells remained viable in the large structure due to printed porosities of the scaffold. Using electrical stimulation, the cardiac cells were observed to contract rhythmically which in turn caused the whole structure to beat periodically. Further development of the model should consider structural integrity of the scaffold to prevent the seepage of fluid from within the structure, as well as the capability to withstand physiological fluid pressures.

Endothelial cells have also been successfully printed with a high degree of accuracy and a precise number of cells per drop.[37] Different methods have been explored for the bioprinting of a 3D vascular network. One method is to print a crosslinking agent (calcium chloride) into an alginate/gelatin solution. The calcium chloride crosslinks the alginate/gelatin solution to form a gelled structure. Boland et al.[38] used this method to produce different structures such as tubes, branched tubes, hollow cones, and capillaries. Using a scanning electron microscope (SEM), the internal structure of the scaffolds was evaluated. It was shown that the calcium chloride crosslinked the alginate/gelatin gel on the surface of the droplet to produce hollow shells. This provided a scaffold with a microscopic porosity. Mouse endothelial cells attached to the surface inside the shells, with filopodia leading into the shells and lamellipodia trailing out, suggesting cell migration into pores.

Another method used for inkjet bioprinting vasculature depended on the reaction between thrombin and fibrinogen to form fibrin. This reaction was used by Cui et al.[7] to encapsulate human microvascular endothelial cells (HMVECs) in a fibrin hydrogel. HMVECs were suspended in a thrombin calcium chloride solution and printed onto a fibrinogen substrate that reacted to fibrin, thus encapsulating the cells. Using this method, scaffolds were fabricated with micron-sized fibrin channels. The printed hollow fibroin channels were well aligned and had a straight microstructure. The average fiber diameter was 93 μm, had an elastic modulus of 2.9 ± 0.8 MPa, an ultimate tensile strength of 1.7 ± 0.5 MPa, and a burst pressure estimated to be 2955 mm Hg; all properties were comparable to that of extruded tissue-engineered blood vessels. After 21 days in cell culture, the cells had aligned along the printed structures to form confluent linings. A ring-shaped microvasculature had formed that had sealed the fibroin channel with a high level of integrity.

One of the issues associated with inkjet printing is the fabrication of overhanging structures. The printing of overhanging structures is challenging as each layer of printed droplets is supported by either the substrate or previously printed layers. To overcome this issue, Christensen et al.[8] used calcium chloride solution for both crosslinking and as liquid support material. Sodium alginate ink, with and without the inclusion of NIH-3T3 mouse fibroblasts, was printed into a calcium chloride solution, which gelled almost instantaneously upon impact. The calcium chloride solution provided buoyancy to the overhanging structures and was easily removed after fabrication, unlike solid support structures that can be difficult to remove post fabrication. The print quality of the rounded overhangs was negatively affected by gravitational forces and droplet impact during printing. The low mechanical integrity of the alginate gel also meant that the designed structure did not maintain its 3D shape during printing. Although the positioning of the walls moved, printing could be compensated to ensure that the structure was completed and the scaffolds exhibited a 90% cell viability after 24 h. The current model would be insufficient for implantation due to the potential for turbulent and vortex blood flows to occur due to poor uniformity of the printed shape. This could induce the development of a thrombosis and eventually block fluid flow.[9] Therefore, due to the poor structural integrity encountered during fabrication related to the use of a liquid support structure, it is suggested that a solid support structure may be preferable when printing a tubular hydrogel scaffold.

Skin tissue. To produce a skin graft, Lee et al.[10,11] printed a layered structure with multiple cell types. Primary adult human dermal fibroblasts (hFB) and primary adult human epidermal keratinocytes (hKC) were suspended in cell media and printed in-between layers of a printed collagen (type I and rat tail) gel.[10] Using a microvalve-based bioprinting system, the number of cells per droplet ranged from 68 ± 13 cells/droplet for hKC to 93 ± 13 cells/droplet for hFB. The inner layers of the scaffold were composed of fibroblasts and the outer layers composed of keratinocytes. There were no morphological differences between the bioprinted cells and manually seeded cells, and no significant difference in cell viabilities. To demonstrate wound-specific scaffold manufacture, scaffolds were printed into polydimethylsiloxane (PDMS) molds with non-planar 3D surface contours. Scaffolds fabricated in the non-planar molds suffered from an inhomogeneous printed layer depth; however, this had no negative influence on the proliferation of the cells.
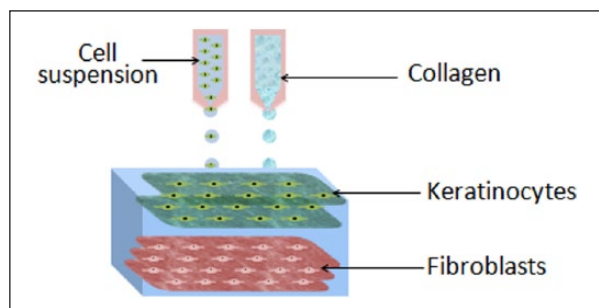
Figure 1. Schematic diagram of multilayered skin tissue with two layers of keratinocytes and three layers of fibroblasts embedded in collagen, fabricated with inkjet bioprinting (taken from a study performed by Lee et al.[11]).

Scaffolds fabricated in the same way but on a planar surface (shown in Figure 1) were compared to conventional scaffolds that required manual seeding of the cells.[11] After 7 days submerged in cell culture medium, the printed scaffolds maintained their shape and dimensions, as well as produced three densely packed cell layers of hKCs on the surface of the scaffold. In contrast, the conventionally produced skin scaffold continually shrunk and had lost shape after 7 days in culture. When exposed to an air–liquid interface, the printed scaffolds developed a dense epidermal layer, with the number of epidermal layers increasing from 3 to 7 after 14 days of cell culture. The epidermal layers formed tight junctions between neighboring cells, an important feature of the epidermis for providing an effective barrier.

An alternative PEG-based skin model has been developed by Rimann et al.[51] Printing at a temperature of 20°C, alternate layers of PEG-based bioink and primary human dermal fibroblasts were deposited to produce a scaffold. Each layer of the PEG-based bioink was immediately polymerized using UV light. The top layers of cells were encased within an additional seven layers of the bioink. DNA damage was measured by the formation of cyclobutane pyrimidine dimer (CPD), a product of UV damage to DNA. UV exposure during printing was shown not to damage cell DNA when compared to unprinted cells. Cell viability, proliferation, and morphology of the printed cells were similar to that of the unprinted cells. After 2 days in cell culture, the fibroblasts were shown to adhere to the printed structure with a typical morphology and spread within the printed matrix. Over a 3-week period, cells continued to proliferate and produce their own extra cellular matrix. Primary human dermal keratinocytes seeded on top of the printed scaffolds did not achieve a fully stratified epidermis when exposed to the air–liquid interface for 14 days. By not printing the keratinocytes onto the scaffold, cell distribution and positioning were affected. Achieving a more uniform layer of keratinocytes during the seeding process could have helped to achieve a stratified epidermis, as demonstrated by Lee et al.[11]

Yanez et al.[52] compared a bioprinted scaffold to a commercial graft (Apligraf®) for treating full-thickness skin wounds in mice. Human dermal microvascular endothelial cells (HMVECs) were suspended in a PBS containing thrombin and calcium chloride. The HMVECs were printed onto a gel consisting of neonatal human dermal fibroblast (NHDF) cells and collagen. After printing and a brief period of incubation, neonatal human epidermal keratinocytes (NHEK) mixed in collagen were applied to the top of the scaffold. Full-thickness wounds were created on the backs of mice, which were then treated with the bioprinted scaffolds, Apligraf®, or treated without a graft. After 14 days, the bioprinted scaffolds had adhered to the wound while the Apligraf had dried out and detached from the implant site, although no infections were recorded for any of the test groups. By Day 21, complete closure of the wound had occurred for the bioprinted scaffold, followed by the Apligraf-treated wounds after 28 days. Wound contraction at all time points was improved in the bioprinted group. By Week 6, the bioprinted group had a wound contraction of $62.5\% \pm 9\%$ compared to the Apligraf with $74\% \pm 5\%$, and the negative control with $79\% \pm 2\%$. All groups developed epidermal and dermal layers; however, the printed skin graft was shown to have the most histologically similar appearance to native skin. The printed scaffold also showed evidence of vascularization, as the printed cells had integrated with the native tissue and helped to develop a microvessel network.

An in-situ printing method has been tested by Skardal et al.[53] Amniotic fluid–derived stem (AFS) cells and bone marrow–derived mesenchymal stem cells (MSCs) were separately suspended in fibrinogen–collagen solutions. The cell suspensions were printed onto full-thickness skin wounds on the backs of mice and crosslinked by printing a separate thrombin solution between layers of the cell suspensions. Only one cell type was used for the treatment of each wound and was compared to scaffolds produced in the same way without the inclusion of printed cells. Printing produced a 100% coverage of the wound with a tight seal between the skin and graft. Wound contraction and re-epithelialization were at all time points significantly higher in the groups with printed cells. After 1 week, wound contraction was 83% for scaffolds with printed cells, compared to 73% for the gel alone. Printed scaffolds exhibited re-epithelialization of up to 89% which had organized, well-defined layers, while the control only exhibited a 51% re-epithelialization with a poor structural quality. Unlike the study of Yanez et al., the printed cells did not integrate with the tissue and had almost disappeared after 7 days. Therefore, in the study conducted by Skardal et al., the benefit of using printed cells was the secretion of trophic factors. The concentration of secreted factors was highest for the AFS cells, which coincided with better regeneration results. Overall, it was determined that AFS cells bioprinted onto a wound site could be

beneficial for burn treatments. This study demonstrates an immediate and practical application of bioprinting. Not only can the graft be printed in situ, the AFS cells could come from a cell bank, enabling the possibility of "off-the-shelf" treatments.

Stem cells. Printing of stem cells presents the potential issue of changing their phenotype, which can be influenced by experimental conditions such as induced shear stresses.[54] The effects of shear stresses on stem cell viability, phenotype, and function were analyzed by Blaeser et al.[55] Over a range of shear stresses, printed primary human mesenchymal stem cells (hMSCs) were shown to have a reduced viability immediately after printing at high shear rates. However, after 7 days in cell culture, no significant difference between cells printed at low and high shear rates was observed. Cell proliferation rate was stimulated by a moderate level of shear stress, yet, above a certain threshold, there was an observed negative effect. Cell phenotype was unaffected by shear forces during printing. The study demonstrated that below a certain shear stress, hMSCs can be printed without side effects.

The effect of printing on other stem cells has also been investigated. Faulkner-Jones et al.[56] investigated the influence of printing on human embryonic stem cells (hESCs) and human-induced pluripotent stem cells (hiPSCs). The use of hiPSCs for tissue engineering applications could be more beneficial than using hESCs, as the hiPSCs could be harvested from the patient and therefore immunosuppressive drugs would not be required for their implantation. The printing process did not change the differentiation of the cells nor change their lineage when compared to unprinted cells. The expression of pluripotency markers was slightly lower than the non-printed cells, however still within an acceptable range. When printing large circular structures, cell viability dropped to 55.5% 1 h after printing; however, the size of the scaffold did not influence the differentiation and maturation process of the cells. A low cell viability of the large scaffolds could be linked to a structural design restricting the availability of nutrients. Another possibility could be extended fabrication time, during which the cells are subjected to non-physiological conditions.

By printing stem cells into a scaffold, it is possible to develop a complex tissue. Gurkan et al.[57] printed MSCs for the development of a multiphase tissue scaffold. Multiphase tissue scaffolds could be useful for repairing soft–hard tissue interfaces such as between tendon and bone. Scaffolds were produced by printing inks composed of methacrylated gelatin (Me-Gel) and hMSC cells, supplemented with bone morphogenic protein-2 (BMP-2), TGF-β1, or a combination of both. Scaffolds were printed with one side containing only BMP-2 and the other only TGF-β1, with a multiphase section in the middle. A smooth transition was produced between each phase. Osteogenesis- and chondrogenesis-related genes were upregulated within the respective BMP-2 and TGF-β1 regions, as well as in the multiphase section after 36 days in culture. Due to the complexity of tissue junctions and the difficulty of producing the intricate organizational structure, there are yet to be any translational studies to test current tissue-engineered scaffolds in a clinical setting.[58] Therefore, the success of bioprinting to differentiate stem cells into different lineages within the same scaffold could be the solution for future development of these complex structures.

Extrusion

Extrusion bioprinting is the most commonly used printing technique and was developed by Scott Crump in the early 1980s and commercialized by his company Stratasys Ltd.[30] An ink is extruded through a printhead to build a 3D shape in a layer-by-layer manner. Extrusion bioprinting is driven by piston, screw, or pneumatic pressure mechanisms. Highly viscous bioinks can be printed through micro-nozzle sizes.[42] Control over the deposition of cells, rate of cell distribution, and process speed have greatly increased the application of this technology for scaffold fabrication.[17,42] The main advantage of this technique is the ability to print very high cell densities with a fast fabrication rate.[18,59] This technique provides excellent structural integrity due to the continuous deposition of the bioink.[60] While extrusion-based bioprinting is already well studied in practice, the current state of the technology has some limitations. Only highly viscous materials can be extruded to maintain filamentous structure after deposition. There are potential cell apoptotic effects induced during and after printing due to a pressure drop associated with extruding through a micro-nozzle.[42] However, this issue can be resolved to an extent by optimizing the process parameters such as material concentration, nozzle pressure, and diameter. The resolution of printing is around 200 μm, which is considerably lower compared to inkjet- and laser-based bioprinting. However, extrusion-based bioprinting can be regarded as a promising technology for tissue regeneration.

Bone tissue. Fedorovich et al.[19] printed intricate porous constructs containing endothelial progenitor cells (EPCs) and multipotent stromal cells (MSCs). Tissue development was studied for scaffolds composed of either Matrigel, or Matrigel and alginate. For the composite scaffold, EPCs were encapsulated in the Matrigel and MSCs in alginate. Scaffolds were implanted into subcutaneous dorsal pockets of mice. The Matrigel scaffolds promoted better cell migration in comparison with the Matrigel–alginate constructs due to fewer interactive properties of alginate. It was found that bone-like tissue had developed in the Matrigel scaffolds at 6 weeks after implantation.[19] However, due to the lower mechanical properties of Matrigel,

load-bearing applications would require the addition of another material construct to provide extra support.

Hung et al.[20] fabricated scaffolds out of PCL and decellularized bone matrix laden with human adipose–derived stem cells (hASCs) for craniofacial regeneration in mice. Compared to a pure PCL scaffold, the composite scaffold had an increased surface roughness. As would be expected with addition of hydroxyapatite, a bioactive material, enhanced bone regeneration was observed with increased cell adhesion in the composite scaffolds compared to pure PCL at 1 and 3 months of post-implantation.[20]

Due to the limited processability of natural polymers, synthetic polymers are often used for bioprinting applications. However, synthetic polymers generally lack similar cellular interactions experienced by natural polymers. In order to attain a more biologically functional 3D-printed scaffold, printed scaffolds comprising PCL, poly(lactic-co-glycolic acid) (PLGA), and β-tricalcium phosphate (β-TCP) were subsequently seeded with human nasal inferior turbinate tissue–derived mesenchymal stromal cells (hTMSCs) to lay down a layer of ECM.[61] After which, the scaffolds were decellularized and prepared for subcutaneous implantation in rats. Compared to printed scaffolds without a layer of ECM, the ECM/PCL/PLGA/TCP scaffolds demonstrated greater osteoinductive potential and an enhanced density of mineralized tissue throughout the defect. Overall, this work demonstrates a potential alternative to xenogeneic or allogeneic bone grafts.

Chondral and osteochondral defects are difficult to treat or reconstruct due to their complicated structure. To date, no clinical methodologies are able to reproduce hyaline cartilage.[21,62] To repair chondral defects, O'Connell et al.[43] introduced a new approach using an "*in-situ* biopen," which can reconstruct chondral, maxilla, and mandible defects. The biopen comprised two ink chambers and an extruder nozzle with a UV source. The biopen enables the deposition of living cells and biomaterials in a manual direct-write fashion. Using the biopen, a human infrapatellar fat pad (IPFP) adipose stem cell–laden gelatin-methacrylamide (GelMA)/hyaluronic acid-methacrylate (HAMa) hydrogel scaffold was fabricated for in-vitro test. It was observed that the viability of biopen-printed cells was 97% after 7 days.[43] The biopen may be limited to be used for simple applications, where a specific structure is not required. For complex tissue structures that rely on the precise positioning of cells and material, using a bioprinting method with a fixed set of axis could prove to be more beneficial.

Cartilage tissue. To meet the increasing demand for cartilage tissue regeneration, Schuurman et al.[44] fabricated a scaffold using GelMA embedded with chondrocytes and PCL to provide structural support. GelMA was also combined with hyaluronic acid to provide an anabolic effect on extracellular matrix synthesis and may be beneficial for cartilage tissue engineering.[29] After printing, cell viability was significantly higher in GelMA/hyaluronic acid hydrogels (82%) compared to GelMA hydrogels (73%). The scaffolds were then implanted in the subcutaneous pockets of nude mice and they observed cartilaginous tissue formation after 4 weeks in both materials.

PCL–alginate gel scaffolds containing chondrocytes were successfully fabricated by Kundu et al. using a multihead deposition system (MHDS). The MHDS had four dispensing heads enabling different biomaterials to be dispensed at the same time.[31] The scaffolds were fabricated using layer-by-layer deposition of PCL followed by a chondrocytes alginate hydrogel bioink. Each layer of the scaffold comprised PCL lines with bioink printed in the gaps between each line. The scaffolds were implanted in the dorsal subcutaneous space of mice. The results indicated the formation of cartilaginous tissue in the scaffold after 4 weeks with 85% cell viability.[31]

Periodontal tissue. Periodontal ligament stem cells (PDLSCs) have great potential for periodontal tissue regeneration.[12] The behavior of PDLSCs after printing was investigated by Ma et al.[63] using GelMA and poly(ethylene glycol) (PEG) dimethacrylate and PDLSCs. Cell viability test showed high viability of 94% after 24 h post printing.

Kim et al.[33] demonstrated a successful reconstruction of maxillary bone in a 12-year-old dog using a printed PCL/β-TCP scaffold. The scaffold was fabricated using micro-extrusion-based 3D bioprinting and demonstrated successful reconstruction 8 months after surgery. This case is believed to be the first case of reconstruction using a 3D-printed scaffold in the maxillary bone defect.[33]

Neural tissue. Autologous grafts are the gold standard for repairing damaged neural tissue. However, such procedures involve high risk due to donor site morbidity, multiple surgery sites, and an increased threat of infection. Hsieh et al. printed neural stem cells (NSCs) embedded in the polyurethane (PU) using fused deposition. The printed scaffolds were studied in a zebra fish traumatic brain injury model.[39] To formulate the bioink, NSCs suspended in culture medium were mixed with PU nanoparticles. The NSC/PU hydrogels promoted the repair of damaged central nervous system in zebra fish. After the implantation with the NSC-laden constructs, nerve function was recovered for the adult zebra fish.[39] This research supports the use of PU for neural grafts have been observed with conventional tissue engineering fabrication techniques.[40]

Owens et al.[64] developed a technology to biofabricate purely cellular nerve grafts using multicellular cylindrical units composed of mouse bone marrow stem cells (BMSCs) and Schwann cells (SC).[59] Scaffolds were fabricated using a multichannel extrusion-based bioprinter (NovoGen MMX; Organovo, San Diego) enabling cellular suspensions to be printed alongside an array of agarose
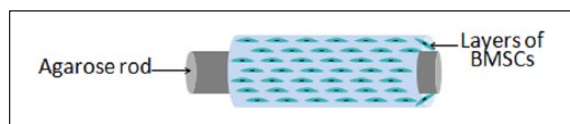
Figure 2. Schematic diagram of a nerve graft fabrication, in which the outer layer is made of bioink containing BMSCs supported by agarose rods. Structures were fabricated with an extrusion-based technique (taken from a study performed by Owens et al.[64]).

rods that provide a temporary support structure (demonstrated in Figure 2). The agarose rod support structure was removed after a maturation period of 7 days. The bioprinted nerve grafts were implanted to bridge a 1-cm gap of the sciatic nerve in rats. The rats recovered both motor and sensory functions at 40 weeks. This study is an excellent representation of the use of bioprinting to aid with scaffold self-assembly for implantation. After a period of 7 days, the cells had produced enough extra-cellular matrix to support themselves and withstand the mechanical forces inflicted during surgery. By implanting only cellular material and cells, the scaffolds more closely represent an autologous graft, which are the gold standard for nerve reconstructive surgeries and currently offer the best option for nerve rehabilitation.

Skin tissue. Lee et al.[10] fabricated a multilayered skin-like tissue structure with the inclusion of fibroblasts and keratinocytes using both extrusion and inkjet printing processes. The cells were suspended in culture medium and printed using an inkjet printhead, while a support structure of poly(dimethylsiloxane) (PDMS) was printed under pneumatic pressure-based extrusion bioprinting. A layer of hydrogel was printed to provide structural integrity for the printed cells. Droplets of cell suspension were dispensed between layers of hydrogel. Each layer of hydrogel was treated with $NaHCO_3$ to induce crosslinking. After printing, the fibroblasts had a viability of 95%, whereas the keratinocytes had a viability of 83.9%. After 8 days of culture, printed fibroblasts showed a higher cell density compared to the keratinocytes. The tissue exhibited better shape retention compared to solid-state scaffold material during in-vitro studies.[10]

Kim et al.[65] demonstrated a 3D bioprinting strategy using an extrusion-based, integrated composite tissue/organ building system (ICBS) bioprinting module to fabricate PCL and collagen-based construct. This printing system provides nine different dispensing modules in which nine different types of biomaterials could be used. Five of the dispensing modules used an extrusion-based printhead, whereas the other four modules used a droplet-based printhead. PCL was extruded as a base mesh construct for an inkjet-printed, collagen-based bioink that contained either human primary dermal fibroblasts (HDFs) or epidermal keratinocytes (HEKs). The samples were cultured in a cell

culture medium for 7 days. The results revealed that the PCL construct with collagen showed biological characteristics such as a fibroblast-stretched dermis and epidermal layers after 14 days, similar to a native human epidermal structure.[65]

Corneal tissue. Corneal transplantation or penetrating keratoplasty (PK) has been a gold standard for the treatment of corneal diseases over the past decades, since Dr Eduard Zirnm performed first cornea transplantation in a human eye in 1905.[66] Limitations of the currently used procedure include the quality of visual recovery due to an increased early endothelial cell loss, detachment of the posterior lamellar grafts, and vascular in-growth into the lamellar plane. Bioprinting technology can replace the limitations of corneal transplantation.

Isaacson et al.[67] fabricated a collagen-based cornea using pneumatic extrusion bioprinting. The bioinks were prepared using sodium alginate and methacrylated type I collagen, mixed with corneal keratinocytes. A plastic support material was printed to help mold the scaffold shape. The support material was printed with a concave hollowed-out structure at the top. The hollowed-out section of the support material was filled with a gelatin slurry in order to support the collagen and alginate bioinks. Cell viability of corneal keratocytes remained was 90% at Day 1 after printing, and 83% after 7 days. Although cell viabilities remained high, a 7% decrease after 7 days could indicate that either the printing process or scaffold design affected the cell survivability. A longer study would be required to evaluate if this was a continuing trend.

Cardiac tissue. Zhang et al.[68] demonstrated a hybrid methodology to fabricate endothelialized myocardium. The construct was fabricated using extrusion bioprinting (NovoGen MMX; Organovo) with multihead dispensing nozzles. Induced pluripotent stem cells (iPSCs) were used to fabricate endothelialized human myocardium. The iPSCs are capable of differentiating into multiple cell lineages including cardiomyocytes. Microfibrous scaffolds were fabricated using GelMA and iPSCs, and seeded with cardiomyocytes to induce the formation of myocardium. It was observed that the printed endothelialized microfibrous scaffold was capable of spontaneous and synchronous contraction.

Duan et al.[69] developed a 3D bioprinted hybrid hydrogel based on methacrylated hyaluronic acid (Me-HA) and Me-Gel to encapsulate human aortic valvular interstitial cells (HAVICs). Cell viability determined using a live/dead assay gave a 90% cell viability. In addition, cells easily adhered and formed a monolayer on the surface of the bioprinted structure, and the encapsulated cells below the surface started to remodel the hydrogel after 3 days in cell culture. Remodeling of the hydrogel is a positive indication for fast graft integration with the host tissue.
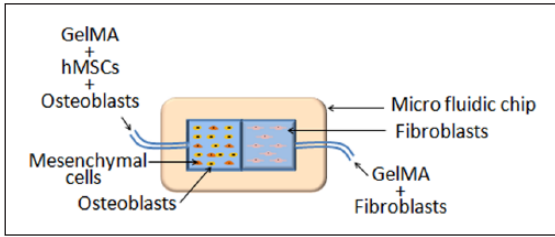
Figure 3. Schematic diagram of a microfluidic chip that mimics bone–tendon junctions, fabricated with pneumatic-based extrusion (taken from a study performed by Miri et al.[72]).

EPCs are known to be a promising cell source for the treatment of ischemic diseases. Gao et al.[70] fabricated a bio-blood-vessel (BBV) using vascular tissue–derived decellularized extracellular matrix (VdECM) and atorvastatin-loaded PLGA microspheres (APMS). Atorvastatin is a proangiogenic drug that promotes endothelial cell function. The BBV was implanted in a nude mouse hind limb ischemia model. Comparing different combinations of BBV, EPCs, and APMSs, it was discovered that BBVs laden with both EPCs and AMPSs significantly increased capillary and arteriole densities.

Jang et al.[71] fabricated a pre-vascularized stem cell patch using a bioink consisting of suspended decellularized porcine heart (dECM), and human c-kit + cardiac progenitor cells (hCPCs), MSCs, or a combination of both cell types. For in vivo testing, PCL was printed as a support for the bioink. Patches were either implanted subcutaneously into mice to test for neovascularization or implanted in a rat myocardial infarction model. The patches improved epicardial activation capability with enhanced angiogenesis. The patterned stem cells promoted strong vascularization and tissue matrix formation with enhanced cardiac functions. Therefore, bioprinted stem cell patches are demonstrated to be a promising therapeutic method for ischemic heart diseases.

Muscular tissue. Miri et al.[72] created hierarchical cell-laden structures to mimic multicellular tissues. Pneumatic extrusion was used to dispense multiple bioinks onto microfluidic chips that were then crosslinked using UV light. In-vitro studies using poly(ethylene glycol) diacrylate (PEGDA) and GelMA loaded with NIH-3T3 fibroblasts, hMSCs, osteoblasts, and C2C12 skeletal muscle cells were printed into structures resembling musculoskeletal junctions, muscle strips, and tumor angiogenesis. The prints retained interfaces and adequate proliferation rates after 3, 5, and 7 days in cell culture. For instance, a microfluidic chip with two different bioinks was fabricated to mimic bone–tendon junctions (Figure 3). The bone side of the chip contained a suspension of osteoblasts and hMSCs in GelMA. The tendon side contained a suspension of fibroblasts in GelMA. To fabricate a tumor angiogenesis resembling model, a microvasculature-like mask was used

during UV curing of PEGDA, followed by washing with PBS and extruding endothelial cell-laden bioink into the microchannels. The interfaces remained explicit and the print patterns were well-defined. For in vivo studies, PEGDA-framed chips that had a concentration gradient of Me-Gel (GelMA) ranging 5%–15 % were implanted subcutaneously in rats. After 30 days, enhanced cell proliferation occurred for 10% GelMA. Having an optimum concentration of 10% GelMA is supported by previous studies performed by Zhou et al.[22,73] and Zhu et al.[74] which will be further discussed later in the review.

Stereolithography

Stereolithography (SLA) is a nozzle-free technique in which the precursor hydrogel is crosslinked via photoirradiation. The process of hardening the hydrogel is called photocuring, which is aided by the addition of photoinitiators. Many parameters are considered during fabrication, such as the type and concentration of photoinitiator, time of light exposure, and type of material. Different types of photoinitiators and their concentrations have been shown to affect cell viability.[75] To eliminate the damaging effects of UV exposure on cells, visible light-sensitive photoinitiators can be utilized. Examples of such initiators are lithium phenyl-2,4,6-trimethylbenzoylphosphinate (LAP),[76] camphorquinone,[23] and eosin Y.[77] Resolution depends on the stereolithographic technology, for example, two-photon SLA has higher printing resolution than single-photon SLA.[24] A printing resolution of 20 μm can be achieved.[78]

Bone and cartilage tissue. The first instance of stereolithographic-fabricated, cell-laden scaffolds were produced by Dhariwala et al.[41] using poly(ethylene oxide) (PEO) and CHO cells. Using SLA, they were able to achieve a print resolution of 250 μm. Cells maintained a good viability and distribution between 1 and 2 days after printing. The scaffolds had insufficient mechanical properties; however, future work could incorporate a second polymer for greater structural strength.

Lu et al.[32] crosslinked PEGDA hydrogels laden with stem cells derived from mouse bone marrow stromal cells (OP-9 cells). The cells remained viable after 24 h. Osteogenic differentiation of mouse mesenchymal stem cells (mMSCs) seeded on to the scaffold showed intensive mineralization after 2 and 4 weeks.

To create biomimetic bone matrices to study metastasis of breast cancer in bone tissue, Zhou et al.[22] employed a table-top commercial stereolithographic printer. The aim was to create a cell-laden 3D structure and seed it with breast cancer cells (BrCas) and observe the interactions in vitro. Currently, most in-vitro cancer studies are performed on monolayered cell cultures which do not accurately mimic the 3D structure of bodily tissues. Osteoblasts and hMSCs were suspended in hydrogels consisting of different concentrations of GelMA and nanocrystalline

hydroxyapatite (nHA). Cell viability of the scaffolds was negatively affected by UV irradiation; however, cell densities increased with time in cell culture. It was found that scaffolds with lower GelMA concentration of 10% exhibited a higher cell viability compared to 15% concentration, suggesting that higher concentrations of GelMA created higher encapsulation stresses and hindered nutrient transport. The osteoblast- and MSC-embedded scaffolds were seeded with BrCa cells and cultured for 2 weeks. After 5 days of culture on 10% and 15% GelMA scaffolds, osteoblast proliferation decreased by 46.9% and 34.7%, respectively, while BrCas proliferation increased by 16.5% and 23.8%, respectively. After 5 days of culture on 10% and 15% GelMA scaffolds, MSC proliferation had also decreased by 37.6% and 30%, respectively, while BrCas increased by 32.5% and 40%, respectively. The decrease in osteoblast and MSC proliferation, and a higher BrCa proliferation, suggests that osteoblasts and MSCs secrete macromolecules that promote BrCas growth which corresponds to other research.[79,80] Vascular endothelial growth factor (VEGF) secretion increased within the 2 weeks, while alkaline phosphates (ALP) activity decreased. As bioprinting techniques develop further, it may be possible to produce more complex biological system and enable the studying of disease interactions not just on a cellular level but also on the surrounding tissue. Building complex tissue models could enable a more accurate study of diseases and even provide a method for the testing of treatments to determine the most effective solutions.

Oxygen inhibition presents a limitation to SLA printing. When SLA is carried out in the presence of air, free radicals from the initiators, used during crosslinking, are seized/scavenged by O_2 molecules. This hinders the polymerization process, impacting print fidelity and ultimately can cause a physical collapse of the scaffold.[81,82] The effect of oxygen inhibition can be reduced by using a high-radiation intensity, increasing photoinitiator concentration, or by performing SLA under inert conditions such as in a nitrogen and carbon dioxide gas atmosphere. However, all of these approaches will negatively impact cell viability.

Lim et al.[13] conducted a study to compare UV and visible light (VIS) crosslinkage of cell-laden hydrogels to minimize the effect of oxygen inhibition. GelMA and bovine collagen I were mixed along with Irgacure 2959 and ruthenium (Ru) + sodium persulfate (SPS) for crosslinking with UV and VIS, respectively. Breast adenocarcinoma cells (MCF-7) were encapsulated in the hydrogels with different concentrations of the photoinitiators to study cytotoxicity effects. It was found that an increase in Irgacure 2959 will affect the cell viability drastically, down to <50% with a concentration of 0.5 wt%, while the different concentrations of Ru/SPS had similar viability rates. To determine the light intensity's effect of UV and VIS on cell viability, a concentration of 0.05 wt% Irgacure 2959 with UV light and 0.2/2 Ru/SPS with visible light were used. The higher the UV intensity, the more the cell viability decreased; however, no significant difference was noted with VIS. Oxygen inhibition was measured by the change in diameter of the printed struts. Printing with VIS-Ru/SPS, the difference in strut diameter was much less than that when using UV-Irgacure 2959, <10%. Further studies were conducted using human articular chondrocytes (HAC) and human bone morrow–derived mesenchymal stem cells (hMSCs), suspended in the GelMA/collagen hydrogels and crosslinked with UV and visible light. Visible light and Ru/SPS exhibited higher cell viability than UV and Irgacure 2959 after 1 day of culture, >85% and <59%, respectively. Irgacure 2959 is a commonly used photoinitiator due to its lower cytotoxicity in comparison with other photoinitiators.[26] As the comparison between cell viabilities of UV and visible light approaches is so stark, the use of visible light may provide the greatest potential for stereolithographic-based bioprinting.

Because of its avascular nature and the presence of low cell densities, cartilage defects will not completely self-regenerate.[83] Zhou et al. included trophic factors into cell-laden cartilage scaffolds to improve cartilage regeneration. hMSCs were combined with 10% GelMA, and different concentrations of PEGDA and PLGA nanospheres containing TGF-β1.[73] Lower concentrations of PEGDA improved cell proliferation after 1, 3, and 5 days. Release studies showed that the nanospheres were able to maintain a sustained release over a 21-day period. After 1, 2, and 3 weeks in cell culture, the expression of chondrogenic genes SOX-9 and Aggrecan were reported to be higher for MSCs in scaffolds containing TGF-β1, suggesting chondrogenic differentiation.

Muscular tissue. Cell patterning and encapsulation were implemented using dielectrophoresis (DEP) and SLA by Bajaj et al.[84] Different cell types, mouse embryonic stem cells (mESCs), and mouse myoblast cell line (C2C12) were patterned and encapsulated in PEGDA hydrogels. Viability rates were similar before and after DEP. After 5 days, live/dead staining showed a slight decrease in cell viability, perhaps because of the non-adhesive property of PEGDA.[25]

Neural tissue. Zhu et al.[74] studied the differentiation potential of human neural stem cells (hNSCs) into neurons after printing using SLA apparatus. Over a range of concentrations, it was determined that low GelMA concentrations yielded higher proliferation rates. 10% GelMA hydrogels were combined with hNSCs and graphene nanoplatelets. Graphene is known to stimulate hNSCs into neural differentiation.[34] Glial fibrillary acidic protein (GFAP) expression is associated with the development of ependymal cells, and β-tubulin III is associated exclusively with neurons and testis cells. After 14 days, β-tubulin III
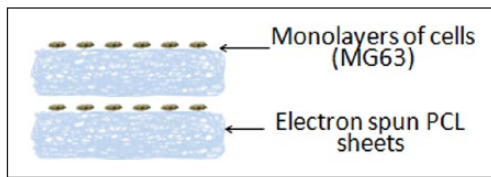
Figure 4. Schematic diagram of consecutive layers of electrospun PCL sheets and monolayers of osteosarcoma cells. Cell placement was controlled using laser-assisted bioprinting (taken from a study performed by Catros et al.[94]).

expression increased while GFAP expression declined. Changes in the expression of GFAP and β-tubulin III, along with neurites elongation, suggest that neural differentiation had occurred.

Laser-assisted bioprinting

Laser-assisted bioprinting (LAB) is a scaffold-free technique that was initially developed in the mid-80s to deposit metal.[85] The apparatus consists of three main parts: (1) a pulsating laser; (2) a donor-slide, to support and propel the printing material; and (3) a receiver-slide, to collect and support the printed material. The technique depends on a laser-induced vaporization effect of a thin layer of gold/titanium that coats the donor-slide. During vaporization, a bubble is created that propels precursor material onto the receiver-slide. When applied to bioprinting, this technique is able to achieve prints with excellent resolution (>20 μm[86,87]) and cell viability. For this process, the precursor material is a hydrogel, which is required to have a mid-ranged viscosity.[5] This technique has been demonstrated to provide accurate multicell positioning.[88] Receiver-slides can be natural (biopapers) or synthetic. Self-assembled cell sheets have also been used for biopapers.[89]

Gudapati et al.[90] studied gelation, gelation time, laser fluence, and their effects on cell viability after print. A bioink consisting of sodium alginate (NaAlg) and NIH-3T3 cells was deposited onto receiving substrates, consisting of either $CaCl_2$ (gelation) or Dulbecco's modified Eagle's medium (DMEM; no gelation). The droplets of NIH-3T3-laden alginate interact with the calcium chloride creating a gelation effect. It was observed that the increase in gelation time and laser fluence resulted in decreased cell viability after 24 h. A gelation time of 2 min created a cushioning effect on the cells, maintaining a better cell viability in comparison with 10 min and no gelation on DMEM, where the cells suffered from irreversible damage. Increased gelation time increased the stiffness of the substrate, hindering nutrient and oxygen diffusion. Ca^{2+} is also known to induce cell injury.[91]

Bone tissue. Biopapers, the biological substrate receivers, are produced to enhance cell viability of LAB prints. Such examples are gelatin, fibrin, alginate, nanohydroxyapatite,

PCL, and PLGA hydrogels. Galbraith et al.[89] developed a self-assembled osseous biopaper using osteogenically differentiated hASCs. Osseous biopapers exhibited higher ALP activity than stromal biopapers after 5, 15, and 21 days. Alizarin red staining displayed higher matrix mineralization within the osseous biopapers. This result is concurrent with current research that indicates that hASCs may be better suited for certain applications in comparison with stromal cells, and that the more easily isolated hASCs may be better suited for LAB-based techniques.[92]

Rapid development of an adequate vasculature within the implanted scaffold is important to avoid hypoxia leading to a necrotic core. Pre-vascularization can be used to improve scaffold regeneration and can be achieved through in-vitro cell seeding and/or in-situ flap techniques. Kawecki et al.[93] performed laser-assisted positioning of human umbilical vein endothelial cells (HUVECs) within the biopapers, as a pre-vascularization step. The endothelial cells were viable immediately after printing. Orientation of the HUVECs showed better alignment for the osseous biopapers. Preservation of cell alignment was favored in the locations where the HUVECs were aligned with cells of the biopapers. After 7 days of printing, tubule-like endothelial cells were observed.

Catros et al.[94] evaluated the effect of 3D positioning of cells on PCL biopapers. The scaffolds consisted of consecutive layers of electrospun sheets and monolayers of osteosarcoma cells (MG63) (demonstrated in Figure 4). For a positive control, the MG63 cells were only printed on top of the scaffolds. Cells were shown to maintain viability after printing. In vitro, cell proliferation rates did not significantly differ between the two groups after 1 and 7 days. However, after 14 days, the scaffolds with the cells printed within the structure exhibited a significantly higher proliferation rate. The scaffolds were implanted in calvarial defects in mice. After 2 months, a significant increase in bone tissue in-growth was observed for scaffolds with organized layers, when compared to the positive control. Histological analysis showed thick fibrous tissue growth in the location of the sequentially layered scaffolds.

Skin tissue. Koch et al.[88] studied the LAB of skin cells; fibroblasts and keratinocytes, and hMSCs. Cell viability immediately after printing was 98% ± 1% and 90 ± 10% for the skin cells, both keratinocytes and fibroblasts, and hMSCs, respectively. Compared to non-printed cells, there was no significant difference in apoptotic activity and proliferation rate between each cell type. hMSCs maintained their phenotype over the course of the study, implying that the transfer process did not induce any up-regulation of surface markers, and hence differentiation.

Corneal tissue. The limbus is an anatomical site that borders the cornea and provides it with limbal epithelial stem cells (LESCs) for regeneration.[95] Destruction of the limbus

by trauma or diseases can deprive the cornea from LESCs and, as a result, cause a limbal stem cell deficiency. Using LAB, Sorkio et al.[96] printed human embryonic stem cell–derived limbal epithelial stem cells (hESC-LESCs) and hASCs for repair of the limbus. Three scaffolds were developed: a stratified corneal epithelium (with hESC-LESCs), a lamellar corneal stroma (with alternating layers of hASCs and acellular bioink), and a scaffold containing both corneal epithelium and stroma. The receiver-slide of the LAB setup contained human-sourced collagen I and recombinant laminin. After printing, the number of cells in each structure tripled after 7 days. Ex vivo assessment of the structures was performed on porcine-excised corneal tissue and compared to acellular Matriderm® sheets as a control. The multicell-laden structures exhibited strong adhesion with the host tissue and hASCs migration to it, while control groups did not exhibit such activities.

Discussion

The four bioprinting techniques have been developed and combined together to produce improved tissue engineering scaffolds and ultimately to replace the current gold standard, autografts. Accurate cell placement has been demonstrated with inkjet printing, as this technique has the capability of printing a singular cell per droplet. Although cell viability is a concern due to the shear stress induced during printing, in practice, it has not been an issue. Inkjet printing has shown great potential for producing skin models that have even been fabricated in situ.[53] Inkjet-fabricated skin grafts have also outperformed a commercial graft Apligraf® in vivo.[52] The flexibility of inkjet printing to print multiple bioinks has been demonstrated by successfully producing complex multiphase tissues.[57] However, this technique is limited in the production of large-scale 3D structures as well as in the printing of over-hanging structures. The problem with printing overhanging structures was encountered when printing a vascular network causing a distortion to the scaffold.[8]

Extrusion-based bioprinting can produce large structures in both horizontal and vertical orientations. It has the capability of printing highly viscous bioinks that contain high cell densities. Extrusion-based techniques vary and have yielded in different cell viabilities; pneumatic-based extrusion has shown to yield higher cell viabilities than mechanical-based. This category of fabrication has shown great potential for chondoral and osteochondoral in-situ applications. The development of a biopen extruder enabled the reconstruction of osteochondral defects with 97% cell viability,[43] demonstrating the great potential for bioprinting to be used directly in a clinical setting.

Stereolithographic bioprinting fabricates scaffolds in a vat of bioink, rather than dispensing the bioink through a nozzle. This exposes the cells to fewer external stresses such as shear forces. Prints have high resolution and generally a smooth surface, however problems can occur with non-polymerized precursor hydrogel becoming trapped within printed 3D porous networks.[97] The main concerns with SLA are the cytotoxicity of the photoinitiators used and UV-induced DNA damaged. To address these issues, visible light-based SLA has been developed and applied in the fabrication of scaffolds.[76] Many investigators have utilized this fabrication technique to obtain a 3D structure that has a homogeneous distribution of one or more cell types. Oxygen inhibition on the photocuring process, hence print fidelity, has not yet been solved, however current solutions include increasing non-toxic photoinitiator concentrations to improve the crosslinking process.[13] Although LAB systems are very expensive, they offer cell-size resolutios. The effect of laser energy inflicted upon cells during printing remains a concern; however, studies have shown that both stromal and stem cells remained viable immediately after printing[88,96] and do not induce any differentiative effect. LAB bioprinting techniques are limited by the scale of tissue scaffolds it can produce due to it being a scaffold-free technique that propels the bioink onto a receiver-slide, usually consisting of a biopaper. These can be natural, synthetic, or even monolayers of self-assembled cells.

Overall, future development of bioprinted tissue scaffolds may require the combination of different printing techniques. Inkjet printing and LAB can provide the most accuracte cell placement, which could be crucuial for the production of complex tissues with multiple cell types. Using inkjet printing, neuronal and glial cells have produced preferential results to seeded cells,[50] indicating the great potential of incorporating a neural network inside a bioprinted tissue scaffold. However, both inkjet printing and LAB are limited by the volume of material that they can dispense and the final mechanical integrity of the printed scaffolds. Therefore, these techniques are required to be combined with other printing techniques to provide a structure with a greater mechanical integrity, such as those produced via extrusion printing. Extrusion bioprinting is a fast method for the production of scaffolds, however there are no guarantees as to cell positioning and distribution within the printed scaffold.

There have been several demonstrations of in-situ application using inkjet and extrusion printing. These have shown an ease of application and fast fabrication times, ideal for translation into a clinical setting. However, some of the current research has encountered problems with producing large, printed structures and the survivability of the cells. This could be related to scaffold design, the extended printing time causing longer exposure of the cells to non-pysiological conditions, or the cell culture method, whereby the use of bioreactors may be necessary. These are all important aspects that need to be explored before bioprinitng can be developed for transferal to clinical applications.

Conclusion

This review has focused on the developmental approaches of bioprinting techniques for the fabrication of different tissues and organs. Bioprinting techniques are gaining substantial interest in the field of tissue engineering due to their ability to create complex structures. Bioprinting enables the production of scaffolds with the precise placement of cells, biomaterials, and biomolecules into spatially predefined locations. Various techniques have been utilized to develop tissues and organs for implantation including blood vessels, cardiac tissues, cornea, and skin. Scaffold vascularization is important for the survival of the implant in situ and has shown great potential for all bioprinting techniques. However, fabricating complex structures with multiple cell types remains a challenge.

Research investigating in situ printing into defect sites has shown promising results, yet, this area of research is still in its infancy. Printing in situ will eliminate any risks of contamination during post fabrication, as well as avoid adverse effects induced by sterilization post fabrication, such as changes to morphology and mechanical integrity of the scaffolds. Organ-on-a-chip is another promising development of bioprinting. It provides the ability for testing multiple cell types without requiring complex models or living systems.

Overall, the choice of fabrication technique depends on the application, type of tissue, and the desired geometry of the print. However, all of the reported techniques hold a great potential to generate fully functional organs.

Declaration of conflicting interests

Funding

ORCID iD

Željka Perić Kačarević https://orcid.org/0000-0002-8250-723X

References

1. Yeong WY, Chua CK, Leong KF, et al. Rapid prototyping in tissue engineering: challenges and potential. *Trends Biotechnol* 2004; 22: 643–652.
2. Stevens B, Yang Y, Mohandas A, et al. A review of materials, fabrication methods, and strategies used to enhance bone regeneration in engineered bone tissues. *J Biomed Mater Res B* 2008; 85: 573–582.
3. Murphy SV and Atala A. 3D bioprinting of tissues and organs. *Nat Biotechnol* 2014; 32: 773–785.
4. Wilson WC Jr and Boland T. Cell and organ printing 1: protein and cell printers. *Anat Rec A Discov Mol Cell Evol Biol* 2003; 272: 491–496.
5. Malda J, Visser J, Melchels FP, et al. 25th anniversary article: engineering hydrogels for biofabrication. *Adv Mater* 2013; 25: 5011–5028.
6. Prendergast ME, Solorzano RD and Cabrera D. Bioinks for biofabrication: current state and future perspectives. *J 3D P Med*. Epub ahead of print 13 October 2016. DOI: 10.2217/3dp-2016-0002.
7. Cui X and Boland T. Human microvasculature fabrication using thermal inkjet printing technology. *Biomaterials* 2009; 30: 6221–6227.
8. Christensen K, Xu C, Chai W, et al. Freeform inkjet printing of cellular structures with bifurcations. *Biotechnol Bioeng* 2015; 112: 1047–1055.
9. Ku DN. Blood flow in arteries. *Annu Rev Fluid Mech* 1997; 29: 399–434.
10. Lee W, Debasitis JC, Lee VK, et al. Multi-layered culture of human skin fibroblasts and keratinocytes through three-dimensional freeform fabrication. *Biomaterials* 2009; 30: 1587–1595.
11. Lee V, Singh G, Trasatti JP, et al. Design and fabrication of human skin by three-dimensional bioprinting. *Tissue Eng Part C-Me* 2014; 20: 473–484.
12. Zhu W and Liang M. Periodontal ligament stem cells: current status, concerns, and future prospects. *Stem Cells Int* 2015; 2015: 972313.
13. Lim KS, Schon BS, Mekhileri NV, et al. New visible-light photoinitiating system for improved print fidelity in gelatin-based bioinks. *Acs Biomater-Sci Eng* 2016; 2: 1752–1762.
14. Xu T, Binder KW, Albanna MZ, et al. Hybrid printing of mechanically and biologically improved constructs for cartilage tissue engineering applications. *Biofabrication* 2013; 5: 015001.
15. Cui X, Boland T, D'Lima DD, et al. Thermal inkjet printing in tissue engineering and regenerative medicine. *Recent Pat Drug Deliv Formul* 2012; 6: 149–155.
16. Cui X, Breitenkamp K, Finn MG, et al. Direct human cartilage repair using three-dimensional bioprinting technology. *Tissue Eng Pt A* 2012; 18: 1304–1312.
17. Ozbolat IT and Hospodiuk M. Current advances and future perspectives in extrusion-based bioprinting. *Biomaterials* 2016; 76: 321–343.
18. Bishop ES, Mostafa S, Pakvasa M, et al. 3-D bioprinting technologies in tissue engineering and regenerative medicine: current and future trends. *Genes Dis* 2017; 4: 185–195.
19. Fedorovich NE, Wijnberg HM, Dhert WJA, et al. Distinct tissue formation by heterogeneous printing of osteo- and endothelial progenitor cells. *Tissue Eng Pt A* 2011; 17: 2113–2121.
20. Hung BP, Naved BA, Nyberg EL, et al. Three-dimensional printing of bone extracellular matrix for craniofacial regeneration. *Acs Biomater-Sci Eng* 2016; 2: 1806–1816.
21. Oussedik S, Tsitskaris K and Parker D. Treatment of articular cartilage lesions of the knee by microfracture or autologous chondrocyte implantation: a systematic review. *Arthroscopy* 2015; 31: 732–744.
22. Zhou X, Zhu W, Nowicki M, et al. 3D bioprinting a cell-laden bone matrix for breast cancer metastasis study. *Acs Appl Mater Inter* 2016; 8: 30017–30026.
23. Tzeng JJ, Hsiao YT, Wu YC, et al. Synthesis, characterization, and visible light curing capacity of polycaprolactone acrylate. *Biomed Res Int* 2018; 2018: 8719624.

24. Weiß T, Hildebrand G, Schade R, et al. Two-photon polymerization for microfabrication of three-dimensional scaffolds for tissue engineering application. *Eng Life Sci* 2009; 9: 384–390.

25. Morris VB, Nimbalkar S, Younesi M, et al. Mechanical properties, cytocompatibility and manufacturability of chitosan:PEGDA hybrid-gel scaffolds by stereolithography. *Ann Biomed Eng* 2017; 45: 286–296.

26. Williams CG, Malik AN, Kim TK, et al. Variable cytocompatibility of six cell lines with photoinitiators used for polymerizing hydrogels and cell encapsulation. *Biomaterials* 2005; 26: 1211–1218.

27. Xu T, Jin J, Gregory C, et al. Inkjet printing of viable mammalian cells. *Biomaterials* 2005; 26: 93–99.

28. Xu T, Gregory CA, Molnar P, et al. Viability and electrophysiology of neural cell structures generated by the inkjet printing method. *Biomaterials* 2006; 27: 3580–3588.

29. Chung C, Erickson IE, Mauck RL, et al. Differential behavior of auricular and articular chondrocytes in hyaluronic acid hydrogels. *Tissue Eng Pt A* 2008; 14: 1121–1131.

30. Pranzo D, Larizza P, Filippini D, et al. Extrusion-based 3D printing of microfluidic devices for chemical and biomedical applications: a topical review. *Micromachines* 2018; 9: 374.

31. Kundu J, Shim J-H, Jang J, et al. An additive manufacturing-based PCL-alginate-chondrocyte bioprinted scaffold for cartilage tissue engineering. *J Tissue Eng Regen M* 2015; 9: 1286–1297.

32. Lu Y, Mapili G, Suhali G, et al. A digital micro-mirror device-based system for the microfabrication of complex, spatially patterned tissue engineering scaffolds. *J Biomed Mater Res A* 2006; 77: 396–405.

33. Kim SE, Shim KM, Jang K, et al. Three-dimensional printing-based reconstruction of a maxillary bone defect in a dog following tumor removal. *In Vivo* 2018; 32: 63–70.

34. Park S, Park J, Sim S, et al. Enhanced differentiation of human neural stem cells into neurons on grapheme. *Adv Mater* 2011; 23: H263–H267, http://onlinelibrary.wiley.com/doi/10.1002/adma.201101503/full

35. Lorber B, Hsiao WK, Hutchings IM, et al. Adult rat retinal ganglion cells and glia can be printed by piezoelectric inkjet printing. *Biofabrication* 2014; 6, 015001.

36. Xu T, Baicu C, Aho M, et al. Fabrication and characterization of bio-engineered cardiac pseudo tissues. *Biofabrication* 2009; 1: 035001.

37. Nakamura M, Kobayashi A, Takagi F, et al. Biocompatible inkjet printing technique for designed seeding of individual living cells. *Tissue Eng* 2005; 11: 1658–1666.

38. Boland T, Tao X, Damon BJ, et al. Drop-on-demand printing of cells and materials for designer tissue constructs. *Mat Sci Eng C* 2007; 27: 372–376.

39. Hsieh FY, Lin HH and Hui Hsu S. 3D bioprinting of neural stem cell-laden thermoresponsive biodegradable polyurethane hydrogel and potential in central nervous system repair. *Biomaterials* 2015; 71: 48–57.

40. Hsu S, Chang W-C and Yen C-T. Novel flexible nerve conduits made of water-based biodegradable polyurethane for peripheral nerve regeneration. *J Biomed Mater Res A* 2017; 105: 1383–1392.

41. Dhariwala B, Hunt E, Boland T, et al. Rapid prototyping of tissue-engineering constructs, using. *Tissue Eng* 2004; 10: 1316–1322.

42. Pati F, Jang J, Lee JW, et al. Extrusion bioprinting. 2015, https://www.sciencedirect.com/science/article/pii/B9780128009727000074

43. O'Connell CD, Di Bella C, Thompson F, et al. Development of the biopen: a handheld device for surgical printing of adipose stem cells at a chondral wound site. *Biofabrication* 2016; 8: 015019.

44. Schuurman W, Levett PA, Pot MW, et al. Gelatin-methacrylamide hydrogels as potential biomaterials for fabrication of tissue-engineered cartilage constructs. *Macromol Biosci* 2013; 13: 551–561.

45. Ink-Jet Printing of Viable Cells. 2003, https://patents.google.com/patent/US7051654B2/en (accessed 28 June 2018).

46. Doyle K. Bioprinting: from patches to parts. *Genet Eng Biotechn N* 2014; 34: 134–135.

47. Zeng M, Jin S and Ye K. Tissue and Organ 3D Bioprinting. *SLAS Technol* 2018; 23: 301–314.

48. Xu C, Zhang M, Huang Y, et al. Study of droplet formation process during drop-on-demand inkjetting of living cell-laden bioink. *Langmuir* 2014; 30: 9130–9138.

49. Shepherd DE and Seedhom BB. The "instantaneous" compressive modulus of human articular cartilage in joints of the lower limb. *Rheumatology* 1999; 38: 124–132, http://www.ncbi.nlm.nih.gov/pubmed/10342624 (accessed 27 August 2018).

50. Tse C, Whiteley R, Yu T, et al. Inkjet printing Schwann cells and neuronal analogue NG108–15 cells. *Biofabrication* 2016; 8: 015017.

51. Rimann M, Bono E, Annaheim H, et al. Standardized 3D bioprinting of soft tissue models with human primary cells. *J Lab Automat* 2016; 21: 496–509.

52. Yanez M, Rincon J, Dones A, et al. In vivo assessment of printed microvasculature in a bilayer skin graft to treat full-thickness wounds. *Tissue Eng Pt A* 2015; 21: 224–233.

53. Skardal SS, Mack A1, Kapetanovic D, et al. Bioprinted amniotic fluid–derived stem cells accelerate healing of large skin wounds. *Stem Cells Transl Med* 2012; 1: 792–802.

54. Tárnok A, Ulrich H and Bocsi J. Phenotypes of stem cells from diverse origin. *Cytom Part A* 2010; 77: 6–10.

55. Blaeser A, Duarte Campos DF, Puster U, et al. Controlling shear stress in 3D bioprinting is a key factor to balance printing resolution and stem cell integrity. *Adv Healthc Mater* 2016; 5: 326–333.

56. Faulkner-Jones A, Greenhough S, King JA, et al. Bioprinting of human pluripotent stem cells and their directed differentiation into hepatocyte-like cells for the generation of mini-livers in 3D. *Biofabrication* 2015; 7: 44102.

57. Gurkan UA, El Assal R, Yildiz SE, et al. Engineering anisotropic biomimetic fibrocartilage microenvironment by bioprinting mesenchymal stem cells in nanoliter gel droplets. *Mol Pharm* 2014; 11: 2151–2159.

58. Baldino L, Cardea S, Maffulli N, et al. Regeneration techniques for bone-to-tendon and muscle-to-tendon interfaces reconstruction. *Brit Med Bull* 2016; 117: 25–37.

59. Marga F, Jakab K, Khatiwala C, et al. Toward engineering functional organ modules by additive manufacturing. *Biofabrication* 2012; 4: 022001.

60. Melchels FPW, Domingos MAN, Klein TJ, et al. Additive manufacturing of tissues and organs. *Prog Polym Sci* 2012; 37: 1079–1104.

61. Pati F, Song TH, Rijal G, et al. Ornamenting 3D printed scaffolds with cell-laid extracellular matrix for bone tissue regeneration. *Biomaterials* 2015; 37: 230–241.

62. Ye K, Di Bella C, Myers DE, et al. The osteochondral dilemma: review of current management and future trends. *ANZ J SURG* 2014; 84: 211–217.

63. Ma Y, Ji Y, Huang G, et al. Bioprinting 3D cell-laden hydrogel microarray for screening human periodontal ligament stem cell response to extracellular matrix. *Biofabrication* 2015; 7: 44105.

64. Owens CM, Marga F, Forgacs G, et al. Biofabrication and testing of a fully cellular nerve graft. *Biofabrication* 2013; 5: 045007.

65. Kim BS, Lee JS, Gao G, et al. Direct 3D cell-printing of human skin with functional transwell system. *Biofabrication* 2017; 9: 025034.

66. Dekaris I. Current trends in corneal transplantation. *Med Sci* 2013; 39: 35–46, https://bib.irb.hr/datoteka/822130. DEKARIS.pdf (accessed 25 June 2018).

67. Isaacson A, Swioklo S and Connon CJ. 3D bioprinting of a corneal stroma equivalent. *Exp Eye Res* 2018; 173: 188–193.

68. Zhang YS, Arneri A, Bersini S, et al. Bioprinting 3D microfibrous scaffolds for engineering endothelialized myocardium and heart-on-a-chip. *Biomaterials* 2016; 110: 45–59.

69. Duan B, Kapetanovic E, Hockaday LA, et al. Three-dimensional printed trileaflet valve conduits using biological hydrogels and human valve interstitial cells. *Acta Biomater* 2014; 10: 1836–1846.

70. Gao G, Lee JH, Jang J, et al. Tissue engineered bio-blood-vessels constructed using a tissue-specific bioink and 3D coaxial cell printing technique: a novel therapy for ischemic disease. *Adv Funct Mater* 2017; 27: 1–12.

71. Jang J, Park HJ, Kim SW, et al. 3D printed complex tissue construct using stem cell-laden decellularized extracellular matrix bioinks for cardiac repair. *Biomaterials* 2017; 112: 264–274.

72. Miri AK, Nieto D, Iglesias L, et al. Microfluidics-enabled multimaterial maskless stereolithographic bioprinting. *Adv Mater* 2018; 30: e1800242.

73. Zhou X, Castro NJ, Zhu W, et al. Improved human bone marrow mesenchymal stem cell osteogenesis in 3D bioprinted tissue scaffolds with low intensity pulsed ultrasound stimulation. *Sci Rep* 2016; 6: 1–12.

74. Zhu W, Harris BT and Zhang LG. Gelatin methacrylamide hydrogel with graphene nanoplatelets for neural cell-laden 3D bioprinting. *Conf Proc IEEE Eng Med Biol Soc* 2016: 2016: 4185–4188.

75. Mondschein RJ, Kanitkar A, Williams CB, et al. Polymer structure-property requirements for stereolithographic 3D printing of soft tissue engineering scaffolds. *Biomaterials* 2017; 140: 170–188.

76. Lin H, Zhang D, Alexander PG, et al. Application of visible light-based projection stereolithography for live cell-scaffold fabrication with designed architecture. *Biomaterials* 2013; 34: 331–339.

77. Wang Z, Abdulla R, Parker B, et al. A simple and high-resolution stereolithography-based 3D bioprinting system using visible light crosslinkable bioinks. *Biofabrication* 2015; 7: 45009.

78. Melchels FPW, Barradas AMC, Van Blitterswijk CA, et al. Effects of the architecture of tissue engineering scaffolds on cell seeding and culturing. *Acta Biomater* 2010; 6: 4208–4217.

79. Weilbaecher KN, Guise TA and McCauley LK. Cancer to bone: a fatal attraction. *Nat Rev Cancer* 2011; 11: 411–425.

80. Goel HL and Mercurio AM. VEGF targets the tumour cell. *Nat Rev Cancer* 2013; 13: 871–882.

81. Studer K, Decker C, Beck E, et al. Overcoming oxygen inhibition in UV-curing of acrylate coatings by carbon dioxide inerting, part I. *Prog Org Coat* 2003; 48: 92–100.

82. Melchels FPW, Dhert WJA, Hutmacher DW, et al. Development and characterisation of a new bioink for additive tissue manufacturing. *J Mater Chem B* 2014; 2: 2282–2289.

83. Hunziker EB. Articular cartilage repair: basic science and clinical progress. A review of the current status and prospects. *Osteoarthr Cartilage* 2002; 10: 432–463.

84. Bajaj P, Marchwiany D, Duarte C, et al. Patterned three-dimensional encapsulation of embryonic stem cells using dielectrophoresis and stereolithography. *Adv Healthc Mater* 2013; 2: 450–458.

85. Bohandy J, Kim BF and Adrian FJ. Metal deposition from a supported metal film using an excimer laser. *J Appl Phys* 1986; 60: 1538–1539.

86. Li J, Chen M, Fan X, et al. Recent advances in bioprinting techniques: approaches, applications and future prospects. *J Transl Med* 2016; 14: 1–15.

87. Dababneh AB and Ozbolat IT. Bioprinting technology: a current state-of-the-art review. *J Manuf Sci Eng* 2014; 136: 061016.

88. Koch L, Kuhn S, Sorg H, et al. Laser printing of skin cells and human stem cells. *Tissue Eng Pt C Me* 2010; 16: 847–854.

89. Galbraith T, Clafshenkel WP, Kawecki F, et al. A cell-based self-assembly approach for the production of human osseous tissues from adipose-derived stromal/stem cells. *Adv Healthc Mater* 2017; 6(4): 1600889.

90. Gudapati H, Yan J, Huang Y, et al. Alginate gelation-induced cell death during laser-assisted cell printing. *Biofabrication* 2014; 6: 035022.

91. Lee GM, Kwan KH, Hoe JH, et al. Effect of calcium chloride treatment on hybridoma cell viability and growth. *Biotechnol let* 1992; 14: 891–896.

92. Strioga M, Viswanathan S, Darinskas A, et al. Same or not the same? comparison of adipose tissue-derived versus bone marrow-derived mesenchymal stem and stromal cells. *Stem Cells Dev* 2012; 21: 2724–2752.

93. Kawecki F, Clafshenkel WP, Auger FA, et al. Self-assembled human osseous cell sheets as living biopapers for the laser-assisted bioprinting of human endothelial cells. *Biofabrication* 2018: 035006.

94. Catros S, Guillemot F, Nandakumar A, et al. Layer-by-layer tissue microfabrication supports cell proliferation in vitro and in vivo. *Tissue Eng Part C Meth* 2012; 18: 62–70.

95. Haagdorens M, Van Acker SI, Van Gerwen V, et al. Limbal stem cell deficiency : current treatment options and emerging therapies. *Stem Cells Dev* 2016; 20161: 979837.

96. Sorkio A, Koch L, Koivusalo L, et al. Human stem cell based corneal tissue mimicking structures using laser-assisted 3D bioprinting and functional bioinks. *Biomaterials* 2018; 171: 57–71.

97. Knowlton S, Yu CH, Ersoy F, et al. 3D-printed microfluidic chips with patterned, cell-laden hydrogel constructs. *Biofabrication* 2016; 8: 1–13.